THE C3PO PROJECT: A LASER COMMUNICATION SYSTEM CONCEPT FOR SMALL SATELLITES

Yann Gouy, Emilie Steck [(1)]
Crisanto Sanchez, Grahame Faulkner, Dominic O'Brien [(2)]
Fabian Sproll, Paul Wagner, Daniel Hampf, Wolfgang Riede [(3)]
Michael Salter, Qin Wang, Duncan Platt, Darius Jakonis, Xiaoyu Piao, Mikael Karlsson, Olof Oberg, Ingemar Petermann [(4)]
Aneta Michalkiewicz, Jerzy Krezel, Anna Debowska [(5)]
Benoît d'Humières [(6)]
Yoann Thueux [(7)]

[(1)] *Airbus Defence & Space SAS, 51-61 route de Verneuil, 78133 Les Mureaux Cedex, France*
[(2)] *Department of Engineering Science, University of Oxford, Parks Road, OX13PJ, UK.*
[(3)] *Institute of Technical Physics, German Aerospace Center, Pfaffenwaldring 38-40, 70569 Stuttgart, Germany*
[(4)] *Sensor System Department, Acreo Swedish ICT AB, Box 1070, 164 40 Kista, Sweden*
[(5)] *Astri Polska Sp. z o.o., Tamka 3, 00-349 Warszawa, Polska*
[(6)] *TEMATYS, 6 cité de Trévise - 75009 PARIS - France*
[(7)] *Airbus Group Innovation, Wellington House, 125 Strand, London, WC2R OAP*

1. INTRODUCTION

The satellite market is shifting towards smaller (micro and nano-satellites), lowered mass and increased performance platforms. This trend is will enable new applications and services as well as innovative space architectures. These applications and architectures have impact on:

- the telecommunications market, providing unprecedented worldwide coverage using constellations with less than 1000 satellites
- the earth observation market, providing
  - responsive earth observation capabilities based on short-lived and expendable small satellites
  - movies delivered using several small satellites queued on the same orbit
- the science market, providing more opportunities for in-orbit experimentations using cost effective platforms and launchers
- the institutional market, potentially replacing unitary satellites by distributed small satellites, increasing architecture robustness and industrialization

The development of these new applications is impacting the design of satellite platforms, resulting in miniaturization, increasing performance, and a reduction of onboard mass, power consumption and volume. In this context, disruptive technologies, such as Electric Propulsion or Laser-optical communication systems, are opening new possibilities. Laser communications is promising since it:

- enables a directive communication link that is secure
- avoids interference,
- does not depend from Radio-Frequency (RF) spectrum regulation
- provides a high data rate,
- offers the potential for power efficiency and mass reduction.

This paper presents the C3PO[1] system, "advanced Concept for laser uplink/ downlink CommuniCation with sPace Objects", and the first results of the development of its key technologies. The objective of the project is to create a communications system that uses a ground based laser to illuminate a satellite, and a modulated retro-reflector to return a beam of light modulated by data to the ground. This enables a simple downlink, without a laser source on the satellite.

This laser communication system is well-suited to small satellites, with the potential to provide a high data rate for very light on-board mass. The aim of the project is to achieve data rates of 1Gbit/s with a transmitter mass of less than 1kilogram.

The C3PO project includes the following activities:

- Design of the system architecture
- Development of the key enabling technologies (Satellite target acquisition, Safety and security, Modulated retro-reflector)
- Demonstrating the system concept through two experiments (acquisition of a satellite target with a laser station and a Gbit/s long distant communication experiment).
-

Current small satellites use RF technology to communicate with the ground station, with VHF, UHF, S, X, Ku, K or Ka band transceivers. The X and K-band can support more than 100Mbps data rates to cubesats, with a mass of few Kgs and an electrical power consumption of few dozens of watts. To give examples, data rates of 150Mbps to 4 Gbps can be achieved for terminal masses of 2.3 to 4kg and power consumption of 30 to 120W[2][3][4] . Besides the data rate and power consumption of these approaches, the growing congestion of the electromagnetic spectrum has led to free space optics (FSO) to become an alternative to RF systems to implement long range point to point high speed data links. FSO laser communication systems have been explored extensively for ground-based communication systems, as well as for in-orbit and interplanetary spacecraft missions. These systems can transfer large amounts of data with a significant decrease in power requirements and hardware mass compared with traditional RF band-based communication systems.
On large satellites, space-to-ground laser communications offer Gbps data rates: more than 5 Gbps have already been demonstrated[5]: The mass of a typical embedded laser communication system is few dozens of kg and its electrical consumption is more than 100W[6].
On CubeSats, several laser-based communication systems are under development, all using laser sources on the satellite: the Aerospace Corporation Optical Communication and Sensor Demonstration (OCSD), with an equipment mass of 3kg and an electrical consumption of 50W, was launched in 2015, with an expected data rate of 5Mbps[6].

[1] C3PO is an H2020 project financed by the European Commission with Grant Agreement: 637595.

[2] L-3com.com, CTX-886 and CTK-830 datasheets
[3] gdmissionsystems.com; HRT150 datasheet
[4] sstl.co.uk, XTx400 datasheet
[5] R. Fields, D. Kozlowski, H. Yura, R.Wong, J. Wicker and C. Lunde, M. Gregory, B. Wandernoth, F. Heine, "5.625 Gbps bidirectional laser communications measurements between the NFIRE satellite and an optical ground station", 2011 International Conference on Space Optical Systems and Applications, 978-1-4244-9685-3/11
[6] R.P. Welle ; S. Janson, D. Rowen, T. Rose, « Cubesat scale laser communications », 31st space symposium, Colorado USA, 2015

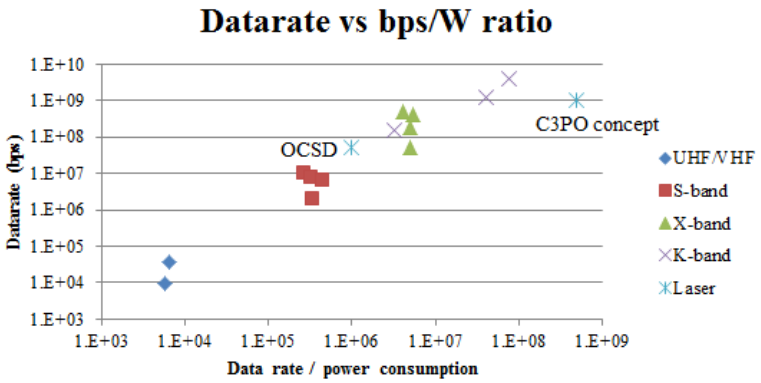

Figure. 1.1: Data rate vs. Data rate/power consumption for different space-to-ground communications technologies.

2. C3PO CONCEPT AND SYSTEM DESCRIPTION

Figure 2.1 and 2.2 show the C3PO system. Each ground-based station is equipped with components used for both uplink and downlink communications: a tracking station for satellite acquisition and pointing and a ground-based laser emitting continuously (for downlink communication) or in a modulated mode (for uplink communication). Downlink communications (figure 2.1) will use a space-based lightweight terminal equipped with a modulated retro-reflector (MRR). This reflects the beam from the ground station and modulates it to send data back to the ground station, where a ground-based optical receiver decodes the data. Uplink communications (figure 2.2) will use an embedded optical receiver on the satellite, receiving the modulated laser signal from the ground.

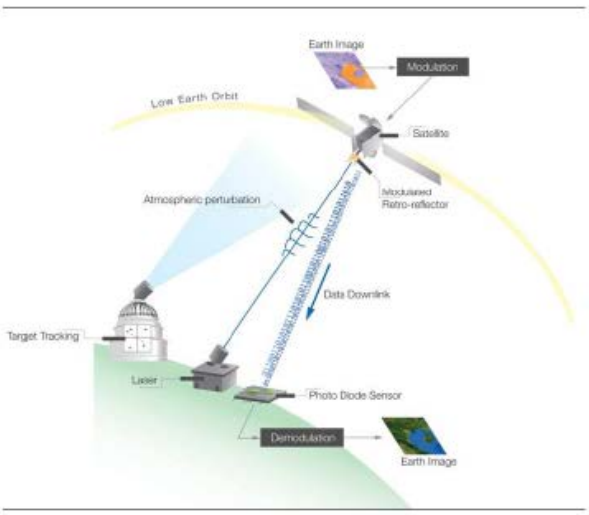

Data downlink mode

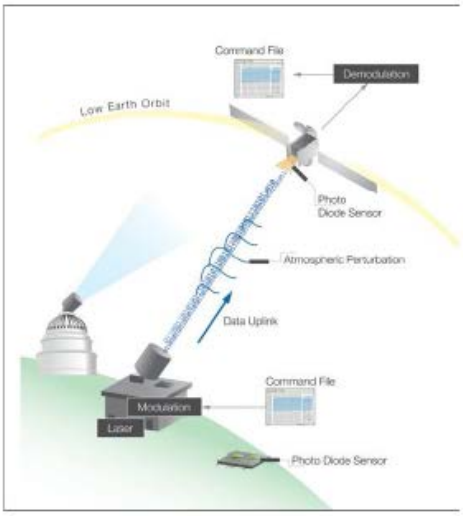

Data uplink mode

Figure 2.1: downlink mode concept (left); Figure. 2.2: uplink mode concept (right)

The C3PO system architecture is composed of three sub-systems:

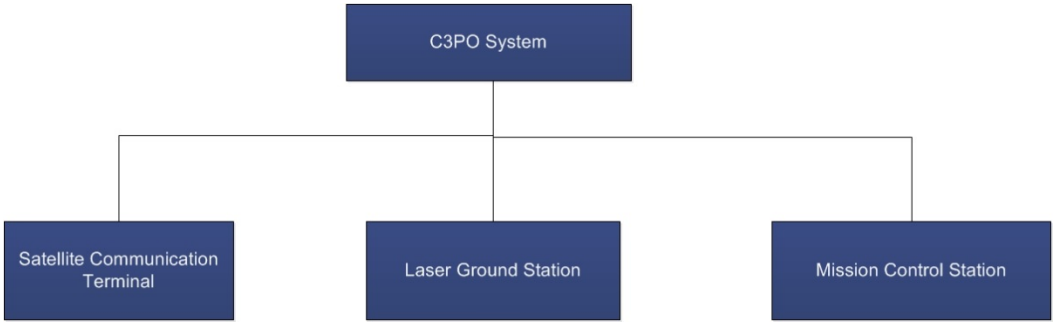

Figure. 2.3: C3PO system architecture concept

- The Satellite Communication Terminal (SCT): a lightweight optical communication terminal embedded on the satellite and allowing laser signal reception, modulation and reflection (the targeted mass is less than 1kg and the electrical power consumption lower than 2W).

- The Laser Ground Station (LGS): a ground-based station that performs the satellite acquisition and pointing, the laser signal emission (modulated for uplink, continuous for downlink) and the laser signal reception.

- The Mission Control Station (MCS): a ground-based station that monitors and controls the set of laser ground stations and dispatches the workload between the available ground stations, in order to acquire all the datasets from the satellites constellation.

The advantages of the C3PO concept, with respect to RF and embedded laser communications systems, are numerous: the SCT is lighter and consumes less power, increasing the data rate to power & mass ratio and allowing heavier payloads for the same missions; the data link is more confined and secure, and less sensitive to electromagnetic interference; the communication link is independent from International Telecommunication Union (ITU) radio spectrum regulation.

There are potential disadvantages, also, but these can be mitigated: the dependence on weather conditions is avoided with the use of multiple LGS supervised by a control center (MSC), allowing transmission and reception of data even in case of local weather conditions at one LGS; the laser safety issue is dealt with by the interface with Air Traffic Management (and any future Space Traffic Management).

3. C3PO PROJECT

C3PO aims to validate these concepts, by developing technologies and techniques and validating them with two field experiments. In the next sections the Modulated Retro-Reflector and tracking algorithm are described.

4. MODULATED RETRO-REFLECTOR

C3PO partner Acreo has over a decade of experience with the development of surface-normal electro-absorption modulators (EAMs) based on multiple quantum wells (MQW) with lateral dimension from 10 µm to 15 mm, operating at up to 10 Gbps,. Thanks to mature III-V technologies, modulator arrays have been successfully demonstrated in the wavelength range from 850 nm and 1550 nm, and these have been used for free-space optical communication and high-speed optical signal processing applications. For example, EAM arrays have been designed and fabricated for enabling light wave architectures for parallel processing of broadband electronic signals in the

optical domain[7]. In addition, EAM arrays have also been used for free space optical links through biological tissue for transcutaneous communication[8].

The modulation principle of the EAM is based on the quantum-confined Stark effect (QCSE), which describes the effect of an external electric field upon the light absorption spectrum of a quantum well (QW). When an electrical field is applied to the QW, two effects appear simultaneously as illustrated in Figure. 4.1. One effect is that the electron and hole-energy levels are moved closer to each other (Stark effect), resulting in an absorption shift to longer wavelengths. Another effect is that the bands tilt and the confined electron and hole related to the exciton are pulled by the electric field in opposite directions, thereby causing the overlap between the electron- and the hole-wavefunction to decrease, broadening the spectrum of the excitonic peak and decreasing its intensity. This shift in the absorption band-edge of the device under electric field can be used to modulate an optical signal at a wavelength close to that edge, by using the field to change the absorption of the material. Based on physical mechanisms behind the electro-absorption modulation we can identify the overall performance of EAMs using their operating bias, contrast ratio, loss, and power consumption as a figure of merit.

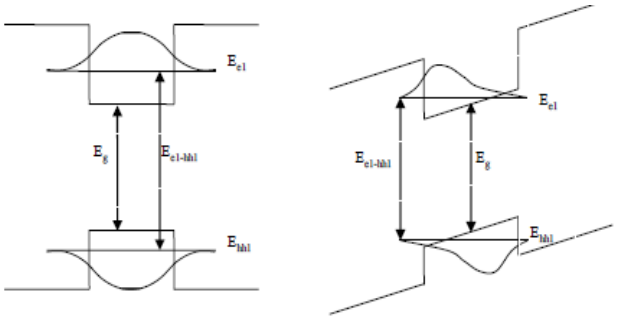

Figure.4.1: Quantum well under electrical field at zero (left) and reverse bias (right)

Surface normal EAMs offer significant advantages in terms of polarisation insensitivity, large active apertures and low insertion losses. A drawback of these modulators is the short interaction length between the incident light and the active medium, which limits the contrast ratio. Single-path surface normal EAMs have typical contrast ratios in the range 2:1.
In the C3PO project, 6x6 EAM arrays operating in the C-band were designed and fabricated using standard semiconductor microfabrication technology at Acreo's ISO-9001 certificated clean-room facilities. The 6x6 EAM arrays are surface normal devices based on InGaAs/InAlAs coupled quantum wells embedded in a pin diode structure with operating wavelength at approximately 1.55 µm. The EAM can operate in a transmissive or reflective mode that uses a metal mirror coated on the EAM's backside[9].

The pixel size of the array is 250 µm x 250 µm with a pitch of 255 µm x 255 µm. To drive each pixels individually a wire-bonding pad (70 µm x 70 µm) was arranged on the top of the pixels, which will block some of the incident optical beam. Thus, the fill factor of the EAM array is about 88.5% including the 5 µm gaps between the pixels and the wire-bonding pad on the top of the pixels. One of the fabricated 6x6 arrays mounted on its PCB is shown Figure. 4.2 (left panel).

---

[7] *Noharet, B., Wang, Q., Junique, S., Ågren, D., and Almqvist, S., ''Multiple quantum well spatial light modulators for optical signal processing'', Photonics and Integrated Optics in RF Systems, Proc. SPIE Vol. 5618 (2004)*
[8] *Mohammad Y Abualhoul, Pontus Svenmarker, Qin Wang, Jan Y. Andersson, Anders J Johansson, ''Free space optical link for transcutaneous communication,'' The International Symposium on Telehealth (Telehealth 2012), 764-048 (2012)*
[9] *Wang, Q., Noharet, B., Junique, S., Almqvist, S., Ågren, D. and Andersson, J. Y., ''1550 nm transmissive/reflective surface normal electroabsorption modulator arrays'', Electronics Letters, Volume 42, Issue 1., (2006)*

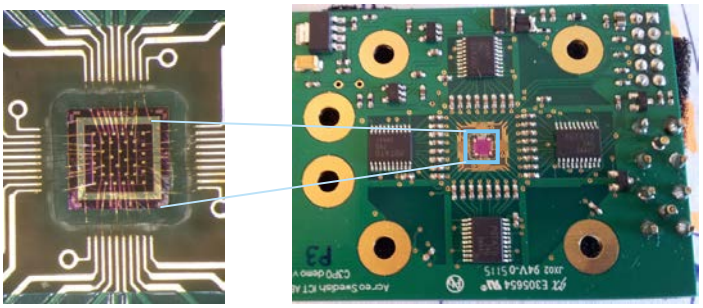

Figure.4.2: A fabricated 6x6 EAM array electrically connected with its driver electronics by wire-bonding

To verify the absorption properties of the fabricated EAM, their transmittance spectra under different reverse bias up to -6 V were measured using a Bruker V80 FTIR spectrometer. The contrast ratio was derived from the transmittance spectra at different biases divided its transmittance at zero bias.

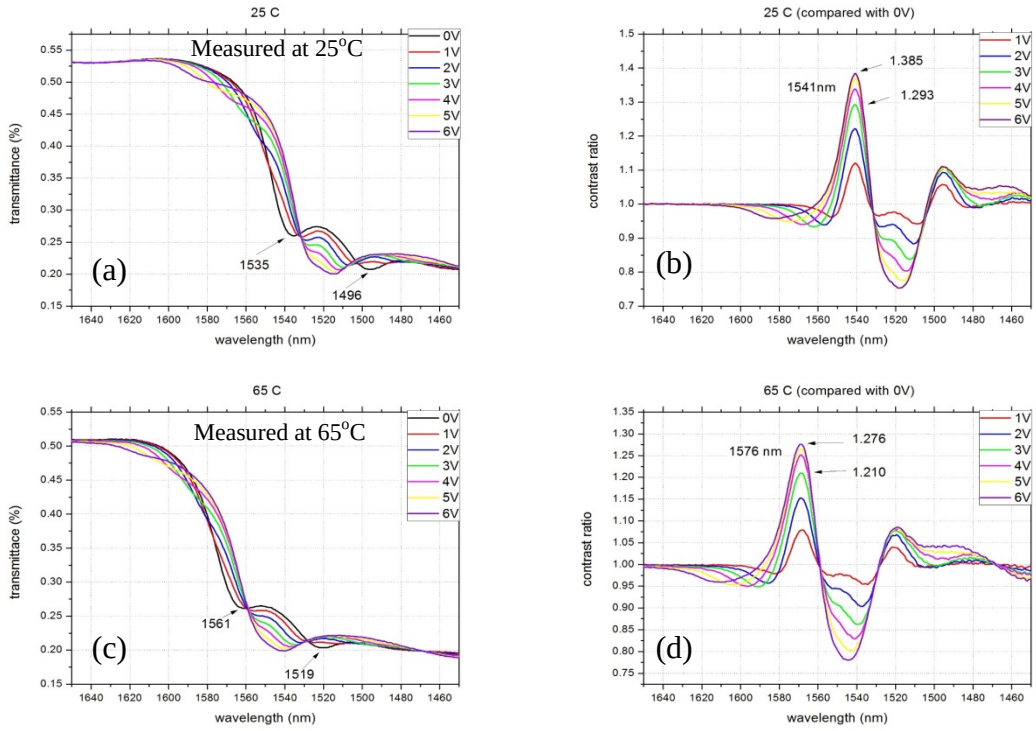

Figure. 4.3 Transmittance spectra and contrast ratio of the EAM array measured by FTIR, at 25°C (up) and 65°C (down), for different biases

The MQW absorption is temperature dependent. To characterize the thermal effect on the EAMs, transmittance spectra were measured for a temperature range from 17°C to 70°C, using a transmissive type EAM. Figure 4.3 (a) and (c) show the transmittance spectra measured at 25°C and 65°C, respectively, and their corresponding contrast ratios as illustrated in Figure 4.3 (b) and (d), respectively. The results reveal clear red-shift of the QW absorption peaks (transmittance dips) with increasing temperature, and about 10% reduction of the contrast ratio at 65°C compared with the 25°C case.

Custom driver electronics was also fabricated by Acreo using commercially available electronic elements and integrated circuits as shown in the Figure 4.2 (right panel). The board has a single LVDS input, and a binary data input signal is used to apply the same modulated voltage to each EAM, thus modulating the contrast ratio. The modulation bandwidth of the EAM array/driver

combination was tested by using a square wave as input to the modulator driver electronics, varying over a frequency range of 10MHz to 500MHz.
The optical response of the fabricated EAMs was characterized. Figure 4.5 shows the optical modulation signals of one of the 6x6 EAM arrays measured at 125 MHz with DC bias at -3.8V at different operating wavelengths of 1541nm (a), 1547nm (b) and 1575nm (c), respectively. An ac (LVDS) signal was applied to the driver PCB by an IDT FemtoClock allowing the generation of up to four different output frequencies ranging from 8kHz to 1GHz. The device temperature was inspected by IR camera during the measurement period, which was in the range from 60^{o}C to 70^{o}C while operating at 125 MHz. Its optical response as shown in Figure 4.5 (d) reveals a good agreement with the contrast ratio profile in the corresponding wavelength range.

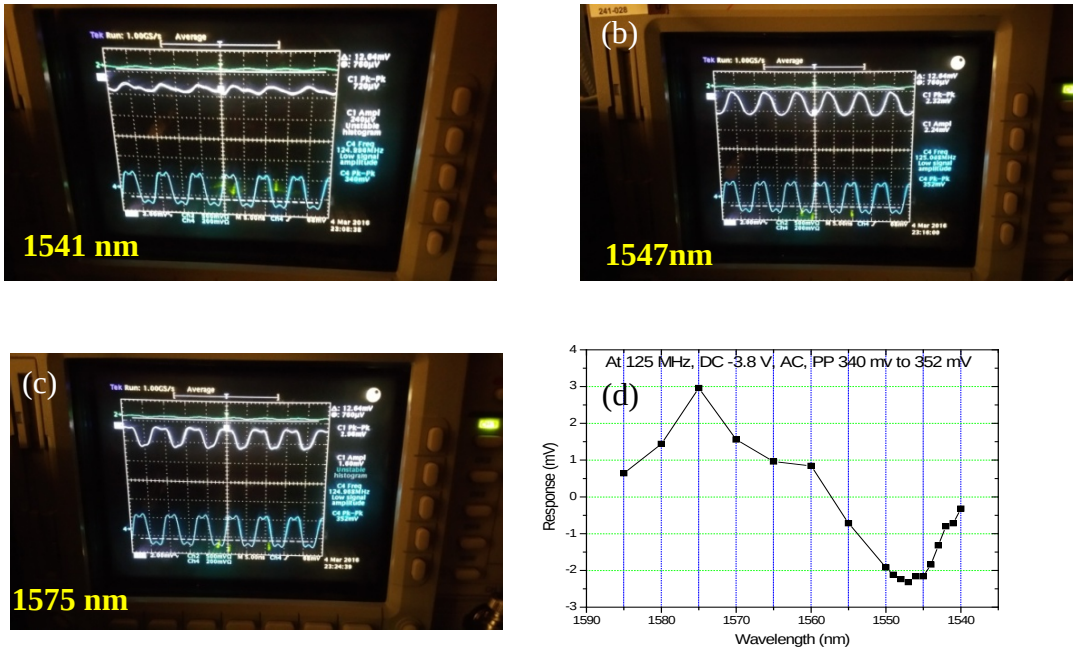

Figure 4.5 Optical modulation signals of one 6x6 EAM arrays at 125 MHz at different operating wavelengths.

At present the driver electronics dissipates significant power, leading to a rise in operating temperature over time, leading to a shift in operating wavelength of the EAMs. This is currently under investigation.

5. TRACKING ALGORITHM

The development of active laser satellite finding and tracking is driven by the need of decreasing the satellite position measurement uncertainty, which is needed for bidirectional ground-space communication using laser beams. Passive optical tracking is realized by observation of the satellite using an optical telescope. After data processing, the position of the satellite can be determined within ±10µrad uncertainty. The goal of the active satellite tracking is to reduce this uncertainty to ±5µrad.
The development of the tracking algorithm requires a numerical model of the tracking process, reflecting specific tracking conditions and reality as far as it can be numerically described. The tracking itself will be conducted at the DLR's observatory in Stuttgart (Germany). This observatory uses a telescope based pulsed laser time-of-flight ranging system that allows accurate location of objects in space (see section 6.1). The tracking algorithm needs to match properties and constraints of observatory's hardware, meeting the tracking requirements at the same time (see Table 5.1).

REQUIREMENT	VALUE	HW PROPERTY	VALUE
Tracking resolution (uncertainty of determination of satellite position)	< 5μrad	Tracking laser beam divergence (initially constant)	120 μrad
		Min tracking beam movement	5 μrad
		Scanning area	2 x 2 $mrad^2$
		Tracking beam's pulse frequency	3 kHz
		Scanning beam step	<5 μrad; 2 mrad>
		Scanning beam step duration regardless step length	1 s
		Beam steering motor moves the spot from point A to point B in 1/3 s, and sets B position precisely in 2/3 s. This means that only 1000 pulses are emitted along the edge scan.	

Table 5.1 Requirements and constraints for the tracking algorithm

The most critical hardware factors affecting the algorithm development are constant tracking beam divergence (unchangeable spot size), scanning step duration and minimum step size. Apart from hardware properties, which can be well characterized, optical turbulence effects the tracking process most, in a random and dynamically changing manner. Deterministic modelling is realized through a set of processes running independently;

- Transmitter: responsible for steering the tracking beam propagating geometrically as a set of pulses; it models also the beam steering motor behaviour.
- Receiver: responsible for counting pulses that hit the telescope aperture, coming from the reflection of the laser by the satellite retro-reflector.
- Satellite: responsible for continuously changing the satellite position with a certain error with respect to the TLE data.
- Algorithm: this process is a client of the transmitter and receiver server.

In the model the stochastic turbulence contribution is realized separately by a statistical characterization of optical turbulence on the beam intensity distribution of the tracking spot (using calculus as well as a scalar wave propagation regime). The results of the statistical analysis are added to the geometrical modelling.

Figure 5.1 shows the base search pattern used by the telescope when locating the satellite. In order to meet the requirements within the optical and mechanical constraints of the system, the tracking algorithm moves the spot along the equilateral triangle edges. The triangle is located so that expected satellite position is in its centre of gravity. Each edge scan (lasting roughly 1 s regardless the edge length, corresponding to 1000 pulses emitted from the telescope ranging system) is considered as a set of detected pulses (AB, BC, CA). The satellite is considered found, if in one scan cycle (A → B → C → A) every set has a pulse count >0. The uncertainty of the satellite position determination is defined by the circle having area equal to the area of intersection of all three sets (AB n BC n CA). This area, the measurement uncertainty, is adjusted by changing the length of the scan edges. If the satellite is found in intersection of only two sets (AB n BC or BC n CA or CA n AB) or in one set only, the triangle is moved in a direction that ensures coverage of triangle centre with satellite position. If the satellite is found in intersection of all three sets, the triangle edges are lengthened (effective area and therefore the uncertainty is decreased). The algorithm is repeated according to Figure 5.2, until the satellite is found with required accuracy.

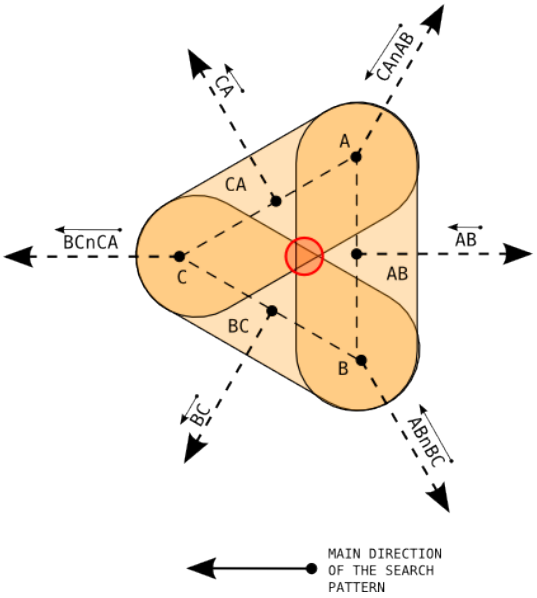

Figure 5.1 The base search pattern

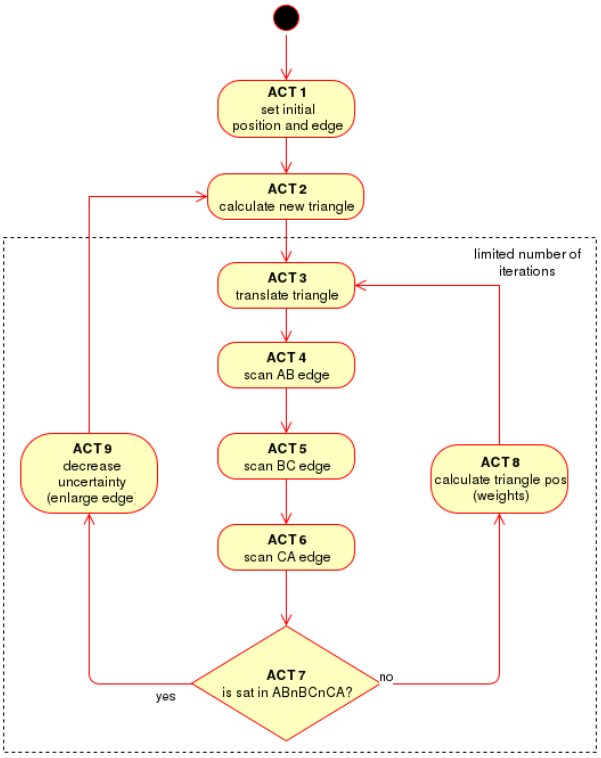

Figure 5.2 The algorithm

The numerical validation of the algorithm is achieved by modelling numerous scanning runs with various initial orientations of the base triangle and the satellite, as well as with various values of optical turbulence strength. In ideal geometrical analyses, the spot position has an uniform distribution of intensity and the probability that the satellite reflects the pulse toward the ground station is 1 inside the search spot, and 0 outside it. In the case of turbulence, each spot has its intensity distribution averaged over 20 samples. Such a distribution defines the probability of pulse reflection and detection (or the energy of returning pulse) by the satellite's retro reflector.
Initial numerical tests of the algorithm show that the satellite can be located in roughly 100 seconds with +/- 5 µrad angular accuracy in an ideal case (geometric regime). Performance of the algorithm using a scalar wave model is currently being performed. Although the modelling covers some important aspects of real operation, the algorithm needs to be validated with a real experiment. This will allow tuning of the algorithm to fit real conditions of operation.

6. DESCRIPTION OF EXPERIMENTS

The aim of the experiments is to obtain measured data, which together will allow the performance of the proposed C3PO system to be predicted. In experiment 1, laser tracking on retro-reflector equipped LEO satellites is performed and the signal strength of the back reflected light is measured in order to assess the real link budget. The main contributions from this experiment concern levels of signal and noise, backscattering effects, tracking accuracy and tracking acquisition time. In experiment 2, an unmanned aerial vehicle (UAV) is equipped with MRR prototypes and laser communication is established with a ground station. The main contributions from this experiment concern the MRR requirements (mass, power consumption), field test operability in usual atmospheric conditions (temperature, rain, humidity) and communication concepts (achievability of a high data rate given a certain signal-to-noise ratio). Each of the experiments is described in more detail in the following subsections.

6.1 FIRST EXPERIMENT: ESTIMATION OF THE LINK BUDGET

In order to estimate the performance of the C3PO system a laser link to LEO satellites will be investigated experimentally. Parameters such as atmospheric backscattering, laser link settle time, minimal elevation of successful laser link and achievable laser link time per pass will be measured. Additionally the link budget will be measured and compared with a theoretical model to assess the communication performance. Therefore, an observation station (see Figure 6.1.1) containing a telescope on an astronomical mount, a laser transmitter as well as dedicated electronics is set up.
Tracking of the target is realized by a coarse pointing of the telescope using the publicly available TLE data and an additional closed loop system for fine tracking. Reflected sunlight from the satellite imaged onto an sCMOS camera is used as input variable to the closed loop system. Tracking accuracies on the order of 10 µrad can be realized with this system[10].
For link budget measurements a Nd:YAG laser operated at the fundamental wavelength (1064nm) with a maximal pulse energy of 300µJ, a FWHM pulse duration of 3ns and a repetition rate adjustable between 1kHz and 10kHz is used. The laser is coupled into a multimode fiber which guides the light onto a laser transmitter directly attached to the tracking telescope. The laser transmitter consists of a beam steering unit enabling a fine steering of the beam with an accuracy of a few µrad over a range of about one mrad. The transmitted beam is expanded to about 6-8cm at the transmitter output.

After propagation through the atmosphere and reflection at the retro reflector equipped target a small part of the infrared light (at the single photon level) is collected by the tracking telescope. A specially designed beam splitter separates the infrared photons from the visible light used for tracking. The infrared light passes a narrow band pass filter for noise reduction and is focused onto an InGaAs based SPAD (single photon avalanche diode) with quantum efficiency up to 30% and a dark count rate below 2kHz.

A dedicated electronic system including an event timer and a GPS receiver for synchronization to UTC is used to measure the time of flight (ToF) of the laser pulse [11]. The differences between the measured and expected ToF as given by the TLE data is computed. This enables the separation of signal events from noise events with a post processing algorithm. Thus the experimental return rate can be extracted.
For calculation of the theoretical return rate the link budget equation as presented in reference [12] can be used for estimating the expected number of generated photo electrons per pulse. With the known (Poisson) detection statistics of the SPAD, the expected return rate can be calculated and compared to the experimental rate.

10 Hampf, Daniel, Paul Wagner, and Wolfgang Riede. "Optical technologies for the observation of low Earth orbit objects." arXiv preprint arXiv:1501.05736 (2015).
11 Humbert, Leif, et al. "Innovative laser ranging station for orbit determination of LEO objects with a fiber-based laser transmitter." CEAS Space Journal (2015): 1-5.
12 Degnan, John J. "Millimeter accuracy satellite laser ranging: a review." Contributions of space geodesy to geodynamics: technology (1993): 133-162.

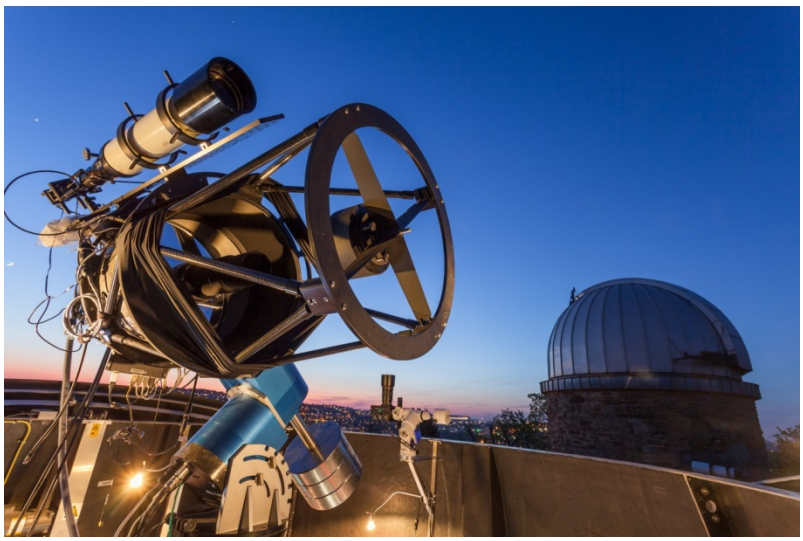

Figure. 6.1.1: The DLR ground station in Stuttgart, Germany will perform link budget measurements to satellites using a pulsed Nd:YAG laser (1064nm, 3ns, 3kHz) as source and an InGaAs based SPAD as detector.

6.2 SECOND EXPERIMENT: LONG-RANGE DATALINK

Experiment 2 targets the implementation of a 1Gbps data link between an unmanned aerial vehicle (UAV) and a base station (BS) using a modulating retroreflector (MRR) including the EAM developed by ACREO. The link range will be at least 1km.

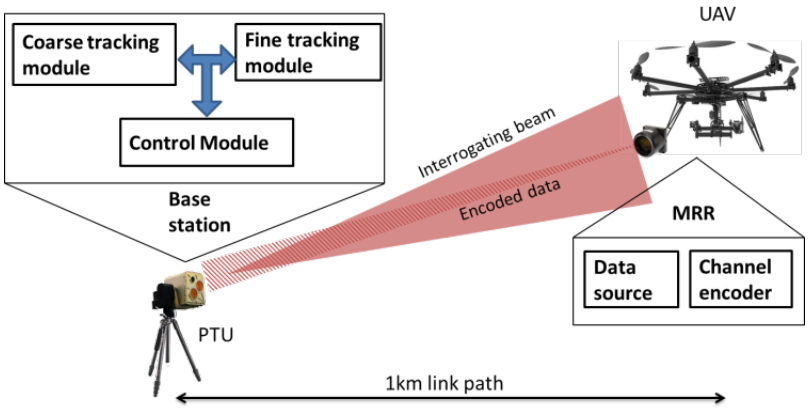

Figure. 3: Experiment 2 system description

Figure 6.2.1 shows the system architecture. A high power Continuous Wave (CW) laser beam is launched from a Base Station (BS) towards a UAV equipped with the Modulator Retro-Reflector (MRR). The UAV position is tracked using both coarse and fine tracking modules working cooperatively. The latter offers a high pointing accuracy within a limited narrow field of view (FOV) of ±0.3°. The system FOV is significantly increased by using a Pan and Tilt Unit (PTU) based coarse tracking subsystem, which mechanically points the BS towards the UAV.

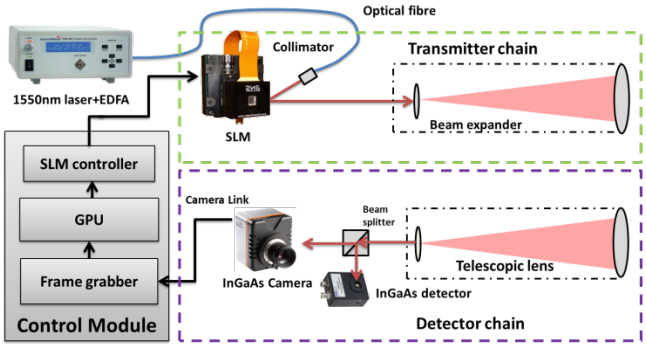

Figure. 6.2.2: Base station optical module

Figure 6.2.2 shows the base station optical module. The system is based on a holographic beam steering module and an InGaAs camera acting as a position sensing device. It is a bi-static design, i.e. the transmitter and receiver do not share the same aperture. The transmitter chain uses a laser source, followed by a spatial light modulator (SLM) which implements beam steering and beam divergence control. After the SLM, an optical beam expander creates an output beam approximately 8cm in diameter. The receiver consists of an 8cm aperture telescopic optical system and a beam splitter that allows the light to be detected by both an InGaAs camera for tracking purposes and a photodetector for the data link.

7. CONCLUSIONS

C3PO aims to show that communications to LEO satellites using MRR based transceivers is feasible, and the project focuses on two experiments that will allow us to do this. Initial results have been obtained from the EAM modulators, a key component, and good progress is being made with the development and integration of other key technologies.